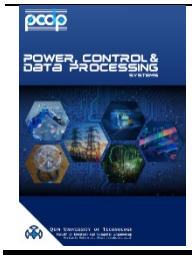
DOI: 10.30511/pcdp.2026.2094243.1096 - ISSN: 3060-8376 - Vol 4(1), 2027



POWER, CONTROL AND DATA PROCESSING SYSTEMS

Available Online at: https://pcdp.qut.ac.ir/

A VIKOR Optimization Approach Towards Predictive Torque Controller Design for Open-End Winding Induction Motors

ARTICLE INFO

Article Type
Original Research

Authors
Vahid Moradi[1]
Khosro Khandani[2]
Mazdak Ebadi[3]

[1] Department of Electrical Engineering, Faculty of Engineering, Arak University, Arak, Iran, moradi.v1994@gmail.com

[2] Associate professor of Electrical Engineering, Department of Electrical Engineering, Faculty of Engineering, Arak University, Arak, Iran, k-khandani@araku.ac.ir

[3] Associate professor of Electrical Engineering Department of Electrical Engineering, Faculty of Engineering, Arak University, Arak, Iran, m-ebadi@araku.ac.ir

* Correspondence
Address: Department of Electrical Engineering, Faculty of Engineering, Arak University, Arak, Iran Postal Code: 71551313.
Phone: +9832625324

k-khandani@araku.ac.ir

Article History
Received: July 12, 2026
Accepted: September 26, 2026
ePublished: March 01, 2027

ABSTRACT

Predictive torque control (PTC) is known as a straightforward approach for induction motor drives for which the control parameters can be directly included in the criterion measure. Nevertheless, choosing the weight factors of the criterion measure is an important challenge. In conventional PTC methods, the criterion measure includes the torque and stator flux control objectives which have different weight factors for each control objective. Tuning weight factors empirically results in a complicated control process. To successfully cope with this issue, this paper suggests the VIKOR method for optimization of the criterion measure. In this research, a new PTC scheme has been proposed using the VIKOR optimization algorithm for the selection of inverter switching vectors connected to an open-end winding induction motor (OEWIM). The purpose of controlling the switching vectors is to reduce the flux and torque ripples. The results are then compared with the conventional PTC and ranking methods. It is demonstrated that, with optimization by the VIKOR method, the flux and torque ripples have been remarkably reduced in comparison with the existing approaches. The proposed VIKOR-based PTC reduces the flux ripple by 78.5% (from 1.4 Wb to 0.3 Wb) and reduces the torque ripple by 58.3% (from 0.012 N·m to 0.005 N·m) compared to the conventional PTC method. Finally, a step-by-step implementation algorithm is presented and simulated using MATLAB which demonstrates favorable results.

Keywords: OEWIM, predictive torque control, VIKOR optimization.

1 Introduction

Variable speed induction motors powered by voltage source inverters have found many applications in industry. Multi-level inverters which are used for precise regulation of flux and torque, have found applications in various fields. This is due to the increase in the number of voltage vectors in such inverters. One of the applications of multi-level inverters is in OEWIMs. Such motors are fed by both sides of the stator windings connected to a multi-level dual-voltage inverter 0 0. One of the major challenges in OEWIMs is how to decrease the ripples of the torque and flux. Various strategies have been introduced to deal with this challenge. For example, model-based predictive approaches have been popular in the literature [2][4]. The most significant feature of predictive control is using the system model to predict the future behavior of the system states. This information is used by a controller according to a predefined optimization criterion to obtain the desired control signal. Additionally, constraints can be included directly in the criterion measure in MPC. MPC has found applications in advanced process control, chemical plants and oil refineries, etc. It has also been used in recent years for torque control of induction motors [5]. This approach is generally referred to as predictive torque control (PTC), in which there is a general need to assign a flux weight coefficient in the criterion measure [6].

Comparing PTC with conventional control methods for OEWIMs such as direct torque control, scalar method, and field oriented control reveals superior performance of PTC [7] [12]. In PTC, a criterion measure is presented which has two constraints of flux and torque control. Since these two constraints are not of the same nature, it is necessary to assign a weight coefficient. There are several offline and online methods to optimize the criterion measure in PTC approaches through adjusting the weight coefficients [13][14]. Offline methods such as aggregation of functions (AOF) and genetic algorithm (GA) are not accurate enough and with the change of working conditions, the optimization must be repeated. In order to alleviate this shortcoming, recent PTC methods have increasingly focused on eliminating heuristic weighting factors while preserving fast dynamic response and high steady-state performance [15]-[17]. Ranking-based MPC evaluates each candidate voltage vector independently for torque and flux objectives and selects the vector with the best aggregate rank, thereby avoiding explicit weighting-factor tuning; however, its computational burden increases as the number of control objectives grows [17]. Additionally, multi-criteria decision-making (MCDM) techniques, including TOPSIS and grey relational analysis, provide a systematic framework for balancing conflicting objectives and have been adopted either for direct vector selection or for weighting-factor optimization, although their implementation complexity remains a concern [18][19]. Among other approaches, normalized weighting methods reduce sensitivity to the scale of different control variables by normalizing objective functions according to their magnitudes or sensitivities, thereby improving robustness and reducing empirical tuning requirements [17]. Other weighting-factor-free strategies include sequential MPC, parallel MPC, equivalent torque-effect methods, reference transformation techniques, and direct vector selection approaches, all of which decouple multiple objectives to avoid scalar weighting [20]. Furthermore, Pareto-based optimization, NSGA-II, entropy-based normalization, and other multi-objective optimization techniques have been investigated to improve the trade-off between torque ripple, flux ripple, switching frequency, and computational complexity, although some methods remain computationally demanding for real-time applications [21]. In [22], VIKOR method for optimizing the criterion measure for a three-phase induction motor has been introduced. In this method which is one of the multi-criteria optimization methods, first of all, two separate criterion measures for flux and torque are considered. Then the minimum and maximum of each criterion measure are calculated. Utility and regret measures have been introduced in VIKOR method which respectively represent the average and worst group scores. The VIKOR index determines the optimal choice from the alternatives which are available [23].

The main goal of this research is to omit the empirical process which is traditionally used for choosing the weight factors in the conventional PTC. Two separate criterion measures are written for each of the flux and torque variables. For each of these criterion measures, a separate weight coefficient is assigned. These weight coefficients are used in the calculation of utility and regret measures in VIKOR strategy. If both flux and torque have ripples, then the weight coefficients are set to 0.5, and if none of the variables have ripples, we consider the weight coefficient equal to zero. In addition, if only one of the variables has ripples, the corresponding weight coefficient is set to one. This linear combination of these two separate functions leads to the selection of an optimal voltage vector which is obtained by calculating the VIKOR index. This is the first work that solves the optimal voltage vector selection problem of an OEWIM drive by VIKOR method. Unlike conventional empirical weighting factors which require tedious trial-and-error tuning, VIKOR provides a mathematical compromise solution that ensures maximum group utility (optimizing both torque and flux simultaneously) while strictly bounding the individual regret (preventing sudden spikes in either torque or flux error). This makes the controller far more robust than the previously published works. Furthermore, while methods like TOPSIS measure the distance to the ideal solution, they do not inherently consider the relative importance of those distances. VIKOR introduces a tuning parameter (the maximum group utility strategy) and actively minimizes the “maximum individual regret”. In the context of motor control, this guarantees that neither the torque nor the flux error exceeds critical limits, making it structurally superior for handling conflicting operational objectives.

While VIKOR has been applied to standard Induction Motors (which have only 8 switching states), the Open-End Winding

Induction Motor (OEWIM) topology driven by dual inverters generates 64 switching states (37 active effective vectors). Using conventional empirical weighting or basic ranking in such an exponentially larger decision-making space becomes computationally exhausting and inefficient. The core novelty lies in proving that VIKOR can mathematically scale to manage the massive 37-vector state-space of OEWIMs efficiently, offering an optimal compromise without the heavy computational penalty that other multi-criteria methods would suffer in this specific dual-inverter topology. A step-by-step algorithm will be proposed to implement the new VIKOR-based PTC strategy. The simulations illustrate that the ripples of the flux and torque are reduced by employing the introduced method.

2 Mathematical Model of the system

In this section the mathematical model of the under-study induction motor is presented.

2.1 Dynamics of the OEWIM

In order to implement PTC strategy, the dynamics of the OEWIM is required. The stationary reference frame has been considered for modelling the OEWIM. The space vector form equations are given as follows [7]:

$$V_s = R_s i_s + \frac{d\lambda_s}{dt} \quad \text{Eq 1}$$

$$0 = R_r i_r + \frac{d\lambda_r}{dt} - j\omega_r \lambda_r \quad \text{Eq 2}$$

where V_s is the vector of the stator voltage, R_r and R_s are respectively the resistances of the rotor and stator; i_r and i_s are also the vectors of the currents of the rotor and stator; λ_r and λ_s are rotor and stator linkage flux vectors, and finally ω_r is the rotor speed of induction motor. The equations of the flux linkages are given by:

$$\lambda_s = L_s i_s + L_m i_r \quad \text{Eq 3}$$

$$\lambda_r = L_m i_s + L_r i_r \quad \text{Eq 4}$$

where L_s *and* L_r are self-inductances of the stator and rotor, L_m is the mutual inductance. The generated torque (T_m) and the fundamental motor-load torque equation are [7]:

$$T_m = \frac{3}{2}\frac{P}{2}\left(imag\{\bar{\lambda}_s \times i_s\}\right) \quad \text{Eq 5}$$

$$T_m - T_l = J\frac{d\omega_m}{dt} \quad \text{Eq 6}$$

where P represents the number of the poles, T_l represents the load torque on motor shaft and and J is the momentum of inertia. With i_s and λ_s as the state variables, the state space equations of the machine model are stated as [7]:

$$\frac{di_s}{dt} = R_1\left(R_2\lambda_s - R_3 i_s + K_r(V_s + Ri_s - j\omega_r\lambda_s) + \frac{j\omega_r i_s}{R_1}\right) \quad \text{Eq 7}$$

$$\frac{d\lambda_s}{dt} = (V_s + Ri_s) \quad \text{Eq 8}$$

Where

$$R = -R_s\,, R_1 = \frac{L_m}{L_s L_r - L_m^2}\,, R_2 = \frac{R_r}{L_m}\,, R_3 = \frac{L_s R_r}{L_m},$$

$$K_r = \frac{L_r}{L_m}\,, V_s = V_{s\alpha} + jV_{s\beta}\,, i_s = i_{s\alpha} + ji_{s\beta}\,, \lambda_s = \lambda_{s\alpha} + j\lambda_{s\beta}$$

The terms ω_m and ω_r in the equations above are respectively the mechanical and rotor speeds.

2.2 Dual Inverter Fed OEWIM

In figure 1, the dual inverter (VSI-1 and VSI-2) connected to the OEWIM is shown [7].

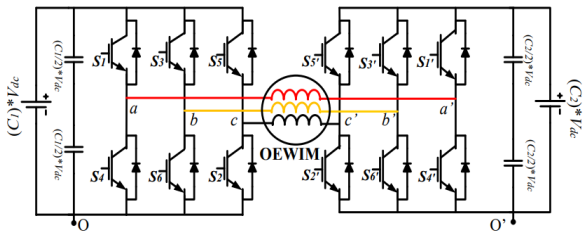


Figure 1: Dual inverter-fed OEWIM [7]

The voltages of poles are represented as [7]:

$$\begin{bmatrix} V_{ao} \\ V_{bo} \\ V_{co} \end{bmatrix} = \begin{bmatrix} S_a \\ S_b \\ S_c \end{bmatrix} \times (C_1 V_{dc}) \quad \text{Eq 9}$$

$$\begin{bmatrix} V_{á\acute{o}} \\ V_{b\acute{o}} \\ V_{c\acute{o}} \end{bmatrix} = \begin{bmatrix} S_{á} \\ S_{b\acute{}} \\ S_{c\acute{}} \end{bmatrix} \times (C_2 V_{dc}) \quad \text{Eq 10}$$

Pole voltages are measured with respect to negative rails of their corresponding VSIs. DC link voltages of dual inverter are maintained in 2:1 ratio so as to obtain four-level inversion. Therefore VSI-1 DC link voltage is set to $C_1 V_{dc}$ where C_1 is 2/3 and $VSI-2$ DC link voltage is set to $C_2 V_{dc}$ where C_2 is 1/3. Sa, Sb, Sc, Sa', Sb' *and* Sc' are the switching pulses applied to the upper switches $(S1, S3, S5, S1', S3', S5')$ of dual inverter. The difference between the voltages of the pole of the dual inverter is defined by (Eq 11). The sum of pole voltage difference in (Eq 12) is not equal to zero.

$$\begin{bmatrix} \delta V_{aá} \\ \delta V_{bb\acute{}} \\ \delta V_{cc\acute{}} \end{bmatrix} = \begin{bmatrix} V_{ao} - V_{á\acute{o}} \\ V_{bo} - V_{b\acute{o}} \\ V_{co} - V_{c\acute{o}} \end{bmatrix} \quad \text{Eq 11}$$

$$\begin{bmatrix} \delta V_{aá} \\ \delta V_{bb\acute{}} \\ \delta V_{cc\acute{}} \end{bmatrix} = \begin{bmatrix} V_{ao} \\ V_{bo} \\ V_{co} \end{bmatrix} + \begin{bmatrix} V_z \\ V_z \\ V_z \end{bmatrix} \quad \text{Eq 12}$$

$$V_z = \frac{1}{3}(\delta V_{aá} + \delta V_{bb\acute{}} + \delta V_{cc\acute{}}) \quad \text{Eq 13}$$

In the current equation, V_z is the zero sequence voltage. By substituting (Eq 13) in (Eq 12), the voltages given to OEWIM phases are:

$$\begin{bmatrix} V_{aá} \\ V_{bb\acute{}} \\ V_{cc\acute{}} \end{bmatrix} = \begin{bmatrix} \frac{2}{3} & -\frac{1}{3} & -\frac{1}{3} \\ -\frac{1}{3} & \frac{2}{3} & -\frac{1}{3} \\ -\frac{1}{3} & -\frac{1}{3} & \frac{2}{3} \end{bmatrix} \times \begin{bmatrix} \delta V_{aá} \\ \delta V_{bb\acute{}} \\ \delta V_{cc\acute{}} \end{bmatrix} \quad \text{Eq 14}$$

3 VIKOR- optimized PTC of OEWIM

Conventional PTC consists of three phases: estimation, prediction and criterion measure minimization to choose the switching state. In this section we present the VIKOR-based PTC where the minimization of the criterion measure is

replaced by VIKOR vector selection stage. All these stages are explained in the following sub-sections.

3.1 Stator Flux Estimation

Considering the Forward Euler's method, the following discretization is applied to obtain the discrete model of the machine:

$$\frac{dZ}{dt} = \frac{Z(k+1)-Z(k)}{T_s} \quad \text{Eq 15}$$

where T_s is the sampling period, $Z(k)$ is any discrete state variable at the instant k. The stator currents (i_a, i_b and i_c) are also measured from the motor phases. Employing Clarke's transformation, they are then converted to two-phase currents (i_α and i_β) in stationary reference frame. With i_α and i_β at hand, the stator current space vector is obtained ($i_s = i_\alpha + ji_\beta$). Then, the PTC algorithm is fed with all the measured values (V_{dc}, ω_r and i_s). Finally, employing Euler's method, the stator flux is estimated as:

$$\lambda_s(k) = \lambda_s(k-1) + T_s((V_s(k-1)) + Ri_s(k-1 \quad \textit{Eq 16}$$

3.2 Prediction of the flux and torque

One-step ahead prediction is applied using all the effective voltage space vectors to obtain $\lambda_s(k+1)$ and $i_s(k+1)$. $Vs1$ and $Vs2$ are respectively the vectors of the voltage space generated from $VSI-1$ and $VSI-2$, for a dual inverter, with an unequal DC link voltages (C_1V_{dc} and C_2V_{dc}) which are given in the following equations:

$$V_{s1} = \left(\frac{2}{3}\right)(C_1 \times V_{dc})\left(S_a + S_b e^{\frac{j2\pi}{3}} + S_c e^{\frac{j4\pi}{3}}\right) \quad \text{Eq 17}$$

$$\mathrm{V_{s2}} = \left(\frac{2}{3}\right)(\mathrm{C_2 \times V_{dc}})\left(\acute{\mathrm{S}}_\mathrm{a} + \acute{\mathrm{S}}_\mathrm{b}\mathrm{e}^{\mathrm{j}2\pi/3} + \acute{\mathrm{S}}_\mathrm{c}\mathrm{e}^{\mathrm{j}2\pi/3}\right) \quad \text{Eq 18}$$

Thus V_s denoting the effective voltage space vector given to the machine is defined as:

$$\mathrm{V_s} = \mathrm{V_{s1}} - \mathrm{V_{s2}} \quad \text{Eq 19}$$

There are 37 effective switching states out of 64 possible dual inverter switching states which are given in Table 1. Then, given the present sample state variables, for all the 37 effective voltage vectors, the stator flux and current are predicted as:

$$\lambda_\mathrm{s}(\mathrm{k}+1)_\mathrm{n} = \lambda_\mathrm{s}(\mathrm{k}) + \mathrm{T_s}\left(\left(\mathrm{V_s(k)}\right)_\mathrm{n} + \mathrm{Ri_s(k)}\right) \quad \text{Eq 20}$$

$$\mathrm{i_s}(\mathrm{k}+1)_\mathrm{n} = \mathrm{i_s}(\mathrm{k}) + \mathrm{T_s}(\mathrm{R_1}\left(\mathrm{R_2}\lambda_\mathrm{s}(\mathrm{k}) - \mathrm{R_3 i_s(k)} + \mathrm{K_r}\left(\left(\mathrm{V_s(k)}\right)_\mathrm{n} + \mathrm{Ri_s(k)} - \mathrm{j}\omega_\mathrm{r}\lambda_\mathrm{s}(\mathrm{k})\right) + \frac{\mathrm{j}\omega_\mathrm{r}\mathrm{i_s(k)}}{\mathrm{R_1}}\right)\right) \quad \text{Eq 21}$$

with n equal to 0 to 36. One-step-ahead motor torque prediction for the effective voltages is:

$$\left(\mathrm{T_m(k+1)}\right)_\mathrm{n} = \frac{3}{2}\frac{\mathrm{P}}{2}\left(\mathrm{imag}\left(\bar{\lambda}_\mathrm{s}(\mathrm{k}+1)_\mathrm{n} \times \mathrm{i_s(k+1)_n}\right)\right) \quad \text{Eq 22}$$

3.3 VIKOR strategy for optimization

In conventional PTC, a criterion measure consisting of the predicted values $(T_m(k+1)_n, \lambda_s(k+1)_n)$ and the corresponding reference values of the control parameters (T_m^*, λ_s^*) is considered to be minimized as:

$$\mathrm{G_n} = \mathrm{w_1}|\mathrm{T_m^*} - \mathrm{T_m(k+1)_n}| + \mathrm{w_2}\left|\lambda_\mathrm{s}^* - |\lambda_\mathrm{s}(\mathrm{k}+1)_\mathrm{n}|\right| \quad \text{Eq 23}$$

The only terms needed to be tuned in the criterion measure are the torque and flux weight factors (w_1, w_2) and selecting them poorly leads to distortions in torque and flux. In this paper, by employing predictive control, we calculate the values of flux and torque for one step ahead $(k+1)$. This means that if torque and flux do not have ripples, then we set the criterion measure coefficients to zero.

If either of flux or torque have ripples, then the corresponding coefficient is equal to one and the other coefficient is set to zero. If flux and torque have ripples, then both coefficients are equal to 0.5. Next, we use the VIKOR method to select the optimal voltage vector. The VIKOR index Q_i determines the optimal choice from the accessible options:

$$\mathrm{Q_i} = \mathrm{v}\left[\frac{\mathrm{S_i}-\mathrm{S^*}}{\mathrm{S^-}-\mathrm{S^*}}\right] + (1-\mathrm{v})\left[\frac{\mathrm{R_i}-\mathrm{R^*}}{\mathrm{R^-}-\mathrm{R^*}}\right] \quad \text{Eq 24}$$

where $S^* = \min S_j$, $S^- = \max S_j$, $R^* = \min R_j$, $R^- = \max R_j$ and v is the group utility factor which is normally chosen as 0.5.

Utility measure denoted by S_i and regret measure represented by R_i are the average and worst group scores. These measures for m alternatives and n criterions are obtained as:

$$\mathrm{S_i} = \sum_{\mathrm{j}=1}^{\mathrm{n}} \mathrm{w_j}\frac{(\mathrm{X_{ij}^*}-\mathrm{X_{ij}})}{(\mathrm{X_{ij}^*}-\mathrm{X_{ij}^-})} \quad \text{Eq 25}$$

$$\mathrm{R_i} = \max_\mathrm{j}\left[\mathrm{w_j}\frac{(\mathrm{X_{ij}^*}-\mathrm{X_{ij}})}{\mathrm{X_{ij}^*}-\mathrm{X_{ij}^-}}\right] \quad \text{Eq 26}$$

where $X_{ij}^* = \max X_{ij}$, $X_{ij}^- = \min X_{ij}$ and w_j is the weight associated with jth criterion. Additionally

$$X_{ij} = \begin{bmatrix} X_{11} & \cdots & X_{1n} \\ \vdots & \ddots & \vdots \\ X_{m1} & \cdots & X_{mn} \end{bmatrix}, X_{ij} = \begin{bmatrix} C_{1S_0} & C_{2S_0} \\ \vdots & \vdots \\ C_{1S_{36}} & C_{2S_{36}} \end{bmatrix},$$

$(C_1)_m = |T_e^* - (T_e^{K+1})_m|$, $and\,(C_2)_m = |\lambda_s^* - (\lambda_s^{K+1})_m|$.

The selection of VIKOR weights is carried out considering the following relation:

$$\sum_{\mathrm{j}=1}^{\mathrm{n}} \mathrm{w_j} = 1 \quad \text{Eq 27}$$

Table 1: Dual inverter effective switching state

$VSI-1$	$VSI-2$	Voltage Space Vector	$VSI-1$	$VSI-2$	Voltage Space Vector
(Sa, Sb, Sc)	(Sa', Sb', Sc')	V_s	(1,0,0)	(1,1,0)	V_{18}
(0,0,0)	(0,0,0)	V_0	(1,0,0)	(0,1,1)	V_{19}
(1,0,0)	(1,0,0)	V_1	(1,0,0)	(0,0,1)	V_{20}
(1,1,0)	(1,1,0)	V_2	(1,1,0)	(0,1,1)	V_{21}
(0,1,0)	(0,1,0)	V_3	(1,1,0)	(0,0,1)	V_{22}
(0,1,1)	(0,1,1)	V_4	(1,1,0)	(1,0,1)	V_{23}
(0,0,1)	(0,0,1)	V_5	(0,1,0)	(0,0,1)	V_{24}
(1,0,1)	(1,0,1)	V_6	(0,1,0)	(1,0,1)	V_{25}
(1,0,0)	(1,1,1)	V_7	(0,1,0)	(1,0,0)	V_{26}
(1,0,0)	(1,0,1)	V_8	(0,1,1)	(1,0,1)	V_{27}
(1,1,0)	(1,1,1)	V_9	(0,1,1)	(1,0,0)	V_{28}
(0,1,0)	(0,1,1)	V_{10}	(0,1,1)	(1,1,0)	V_{29}
(0,1,0)	(1,1,1)	V_{11}	(0,0,1)	(1,0,0)	V_{30}
(0,1,0)	(1,1,0)	V_{12}	(0,0,1)	(1,1,0)	V_{31}
(0,1,1)	(1,1,1)	V_{13}	(0,0,1)	(0,1,0)	V_{32}
(0,0,1)	(1,0,1)	V_{14}	(1,0,1)	(1,1,0)	V_{33}
(0,0,1)	(1,1,1)	V_{15}	(1,0,1)	(0,1,0)	V_{34}
(0,0,1)	(0,1,1)	V_{16}	(1,0,1)	(0,1,1)	V_{35}
(1,0,1)	(1,1,1)	V_{17}	(1,0,0)	(0,1,0)	V_{36}

In this paper, two separate criterion measures are written for each of the flux and torque variables. For each of these criterion measures, a separate weight coefficient is assigned. These weight coefficients are used in the calculation of utility and regret measures in (Eq 25) and (Eq 26). If both flux and torque have ripples, then the weight coefficients are set to 0.5. If none of the variables have ripples, we consider the weight coefficient equal to zero, and if only one of the variables has ripples, the corresponding weight coefficient is set to one. The implementation procedure of the proposed method is summarized as the following steps:

Step 1: Measure V_{dc}, i_s and ω_r. Then apply the optimal switching state S_{opt}.

Step 2: Estimate $\lambda_s(k)$.

Step 3: Predict $\lambda_s(k+1)$ and $T_e(k+1)$ for all switching vectors in (20) and (22).

Step 4: Obtain VIKOR index (Q_i) in (24).

Step 5: Obtain S_{opt}.

The presented step-by-step algorithm shows the proposed strategy is convenient to implement. Now, to demonstrate the effectiveness of the method in the reduction of flux and torque ripples, several simulations are done which are presented in the following section.

Remark 1. The dynamic assignment of weight coefficients in the proposed method acts as a discrete supervisory boundary control. When both torque and flux ripples are out of limits, equal group utility ($v = 0.5$) is mandated to ensure unbiased convergence toward the reference.

Remark 2. Since VIKOR relies on simple algebraic operations and normalizations rather than complex iterative loops, the increase in memory footprint and execution time is marginal, ensuring it is entirely feasible for real-time online execution.

4 Simulation Results and Discussion

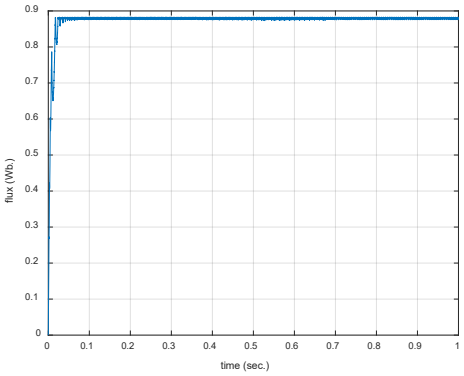
MATLAB/Simulink has been employed to simulate the results. The parameters of the induction motor are given in Table 2.

Table 2: OEWIM Specifications

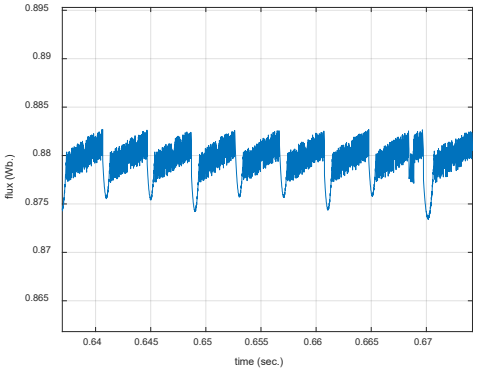
Motor Parameter	Symbol	Quantity
Stator Resistance	R_S	4.2 Ω
Rotor Resistance	R_r	2.6 Ω
Stator Inductance	L_s	0.54 H
Rotor Inductance	L_r	0.54 H
Mutual Inductance	L_m	0.512 H
Poles	P	4
Inertia	J	0.031 kg-m^2
Rated Power	P_n	3.7 KW
Rated speed	N_r	1440 RPM
Voltage line	V_L	400 V

The proposed method was evaluated at a reference speed of 120 rad/s and its performance was compared with conventional PTC and the ranking-based PTC method [11]. The comparison focuses primarily on stator-flux ripple, electromagnetic torque ripple, speed tracking, and stator-current behavior. The proposed controller predicts the stator flux and current for all 37 effective voltage vectors generated by the dual-inverter configuration and predicts the corresponding electromagnetic torque one sampling step ahead. The VIKOR procedure then evaluates the candidate vectors according to the torque- and flux-error criteria and selects the voltage vector that provides the most appropriate compromise between the competing control objectives. This procedure avoids the need for fixed empirically tuned weighting factors in the conventional PTC criterion.

Figure 2 presents the stator-flux response of the proposed PTC, with Figure 2(a) showing the overall response and Figure 2(b) providing a magnified view of the flux ripple. The results show that the stator flux remains centered around its reference value during the simulated operating interval. Although a small periodic variation remains because of the discrete nature of the predictive control process, the magnitude of this variation is relatively small.



(a)



(b)

Figure 2: Flux Ripples in the Proposed PTC a) zoomed out b) zoomed in

Table 3 provides a direct assessment of the flux-ripple performance. At the reference speed of 120 rad/s, the conventional PTC produces a flux ripple of 1.40 Wb, whereas the ranking-based PTC produces 1.25 Wb. With the proposed VIKOR-based PTC, the flux ripple is reduced to 0.30 Wb. Thus, relative to conventional PTC, the reported flux-ripple magnitude is reduced by approximately 78.6%. Compared with the ranking-based PTC, the reduction is approximately 76.0%. This reduction is related to the multi-objective voltage-

vector selection mechanism used in the proposed controller. In conventional PTC, the criterion function contains separate weighting factors for torque and flux errors, and inappropriate selection of these factors can distort the relative regulation of the two variables. In the proposed method, the criterion coefficients are selected according to the presence of torque and flux ripples. When both quantities exhibit ripple, equal weighting is assigned to the two objectives, and the VIKOR procedure subsequently considers both the overall utility and the worst individual criterion.

Table 3: Comparison of torque ripple, flux ripple achieved in the proposed PTC of OEWIM drive with existing methods

Control Method	Speed (rad/s)	Flux Ripple (Wb)	Torque Ripple (N.m)
Conventional PTC	120	1.4	0.012
PTC based Ranking	120	1.25	0.01
Proposed PTC	120	0.3	0.005

Figure 3 shows the electromagnetic torque response obtained using the proposed PTC. The torque remains close to its desired operating value, while the high-frequency oscillations associated with predictive switching are limited. The figure therefore demonstrates the ability of the proposed controller to maintain torque regulation while reducing the instantaneous torque variations.

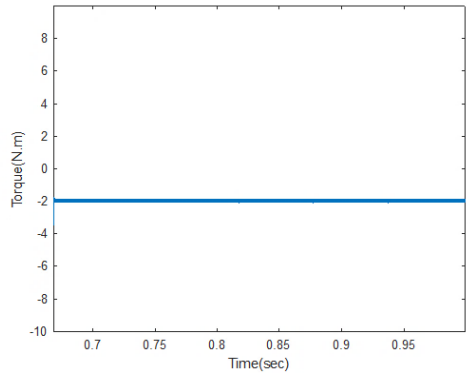


Figure 3: Torque Ripple in Proposed PTC

The numerical values in Table 3 further support this observation. The torque ripple is 0.012 N·m for conventional PTC and 0.010 N·m for the ranking-based PTC, whereas the proposed VIKOR-based PTC reduces the reported torque ripple to 0.005 N·m. The reduction relative to conventional PTC is therefore approximately 58.3%, while the reduction relative to the ranking-based method is 50%.

Figure 4 illustrates the speed response of the OEWIM. The motor reaches the specified operating speed of 120 rad/s and follows the commanded speed trajectory during the simulated operating interval. The response indicates that the reduction in torque and flux ripple does not prevent the controller from producing the electromagnetic torque required for speed regulation.

Figure 5 presents the stator-current response of the OEWIM. The current waveform exhibits transient changes associated with changes in the operating condition and a comparatively repetitive behavior during intervals in which the speed remains approximately constant. This behavior is consistent with the role of stator current in establishing both the stator flux and electromagnetic torque.

The current response is also directly related to the predictive nature of the proposed controller. For each sampling interval, the stator current and flux are predicted for all 37 effective voltage vectors, and the corresponding electromagnetic torque is calculated. The voltage vector selected through the VIKOR index consequently affects the subsequent current trajectory.

The relatively stable current behavior during constant-speed intervals is consistent with the corresponding torque and flux responses. During speed transitions, however, the current changes as the controller modifies the electromagnetic torque to produce the required change in rotor speed. Thus, the current waveform provides an additional indication that the proposed controller responds to changes in the operating condition rather than maintaining a fixed voltage-vector selection.

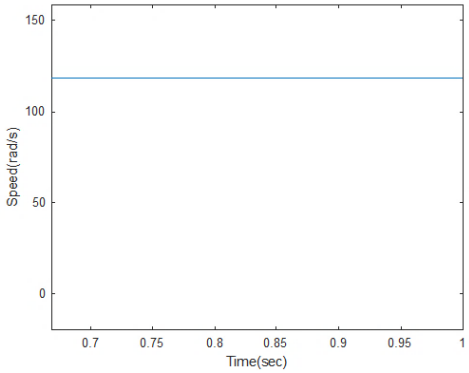


Figure 4: Speed of the OEWIM

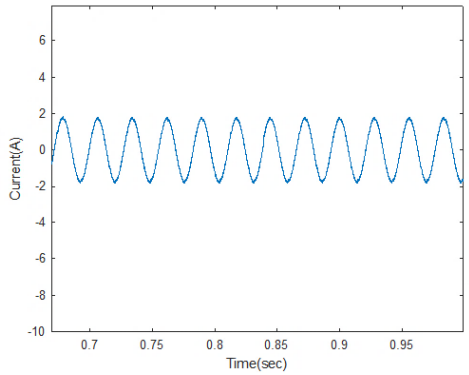


Figure 5: Current of the OEWIM

Figure 6 presents the variations of electromagnetic torque and stator flux with respect to changes in motor speed. This figure is particularly important because it illustrates the interaction between the electrical and mechanical variables of the drive.

During the speed transitions, the electromagnetic torque changes in response to the required acceleration or deceleration of the rotor, whereas the stator flux remains approximately close to its reference value. When the rotor

speed becomes approximately constant, the acceleration approaches zero and the electromagnetic torque approaches the load torque. Consequently, the torque response varies during speed transitions but becomes comparatively steady once the speed reaches a constant operating condition.

The results also demonstrate that speed regulation is achieved without producing large deviations of the stator flux from its reference value. This is an important feature of the proposed multi-objective control strategy because flux regulation and torque regulation are not independent objectives. The predictive controller must select voltage vectors that simultaneously influence both variables. The VIKOR strategy addresses this interaction by evaluating the predicted torque and flux errors using the utility and regret measures before selecting the voltage vector.

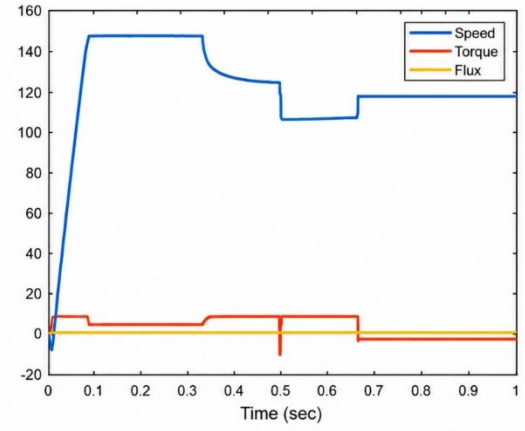


Figure 6: Changes of Torque and Flux with respect to speed changes

Figure 7 shows the stator-current variation corresponding to the speed changes. The current changes during acceleration and deceleration and becomes comparatively steady when the rotor speed reaches an approximately constant value. This behavior follows the changes observed in electromagnetic torque and is consistent with the electromechanical coupling of the induction motor.

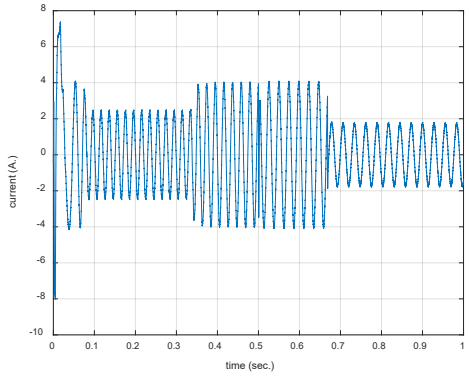


Figure 7: Changes of current with respect to speed changes

During a speed transition, an electromagnetic torque different from the load torque is required to change the rotor speed. The corresponding change in torque is accompanied by a change in stator current. Once the speed becomes approximately constant, the required acceleration becomes small and the electromagnetic torque approaches the load torque; consequently, the current also becomes more stable.

The response in Figure 7 therefore confirms that the proposed controller is able to modify the electrical state of the OEWIM according to changes in the mechanical operating condition. At the same time, the current response remains consistent with the approximately constant stator-flux behavior shown in Figure 6. The results indicate coordinated regulation of current, flux, torque, and speed rather than independent regulation of individual variables.

5 Conclusion

This paper introduced an optimized predictive torque and flux control method for OEWIM drives. The proposed method provides a simple control mechanism without any extra complicated calculations and alleviates the issues encountered when using classical PTC for OEWIM drives. In this paper, VIKOR method was used for the minimization of the criterion measure to select the best voltage vector. This method eliminates the complicated process of empirical selection of the weighting factors. The comparison with existing methods illustrates the superiority of the proposed approach. The proposed method reduced the flux ripple by 78.5% the torque ripple reduction was 58.3% compared to the conventional PTC method. Our future research will focus on the real-time hardware implementation of the proposed VIKOR-based PTC using FPGA platform to experimentally validate its performance under real-world conditions.

Disclosure of Potential Conflicts of Interest

The Authors declare that there is no conflict of interest

Reference

[1] Aisyah, N., Azri, M., Jidin, A., Aihsan, M. Z., & Talib, M. (2021). A New Optimal DTC Switching Strategy for Open-End Windings Induction Machine using Dual Inverter. *International Journal of Power Electronics and Drive Systems*, *12*(3), 1405. doi: http://doi.org/10.11591/ijpeds.v12.i3.pp1405-1412

[2] Kumar, K. V. P., & Kumar, T. V. (2017). Predictive torque control of open-end winding induction motor drive fed with multilevel inversion using two two-level inverters. IET Electric Power Applications, 12(1), 54-62. doi:10.1049/iet-epa.2017.0209

[3] Eswar, K. M. R., Kumar, K. V. P., & Kumar, T. V. (2018). A Simplified Predictive Torque Control Scheme for Open-End Winding Induction Motor Drive. IEEE Journal of Emerging and Selected Topics in Power Electronics, 7(2), 1162-1172. doi:10.1109/JESTPE.2018.2832240

[4] Anunciya, J. D., & Sivaprakasam, A. (2022). A computationally efficient torque and flux ripple reduction by active vector optimization approach using direct torque control–based model

predictive torque control for matrix converter–fed permanent magnet synchronous motor. Transactions of the Institute of Measurement and Control, 44 (9), 1887-1903. https://doi.org/10.1177/01423312211068811

[5] Eswar, K. M. R., Kumar, K. V. P., & Kumar, T. V. (2018). Modified predictive torque and flux control for open end winding induction motor drive based on ranking method. IET Electric Power Applications, 12(4), 463-473. doi: 10.1049/iet-epa.2017.0679

[6] Rojas, C. A., Rodriguez, J. R., Kouro, S., & Villarroel, F. (2016). Multiobjective fuzzy-decision-making predictive torque control for an induction motor drive. IEEE Transactions on Power Electronics,32(8),6245-6260. https://doi.org/10.1109/TPEL.2016.2619378

[7] Meesala, R. E. K., Kunisetti, V. P. K., & Thippiripati, V. K. (2018). Enhanced predictive torque control for open end winding induction motor drive without weighting factor assignment. IEEE Transactions on Power Electronics, 34(1), 503-513. https://doi.org/10.1049/iet-pel.2018.5599

[8] Rojas, C. A., Rodriguez, J., Villarroel, F., Espinoza, J. R., Silva, C. A., & Trincado, M. (2012). Predictive torque and flux control without weighting factors. IEEE Transactions on Industrial Electronics, 60(2), 681-690. https://doi.org/10.1109/TIE.2012.2206344

[9] Kunisetti, V. P. K., Meesala, R. E. K., & Thippiripati, V. K. (2017). Improvised predictive torque control strategy for an open end winding induction motor drive fed with four-level inversion using normalised weighted sum model. IET Power Electronics, 11(5), 808-816. https://doi.org/10.1049/iet-pel.2017.0594

[10] Hannan, M. A., Ali, J. A., Mohamed, A., & Hussain, A. (2018). Optimization techniques to enhance the performance of induction motor drives: A review. Renewable and Sustainable Energy Reviews, 81, 1611-1626. https://doi.org/10.1016/j.rser.2017.05.240

[11] Alsofyani, I. M., & Idris, N. R. N. (2013). A review on sensorless techniques for sustainable reliablity and efficient variable frequency drives of induction motors. Renewable and sustainable energy reviews, 24, 111-121. https://doi.org/10.1016/j.rser.2013.03.051

[12] Vasudevan, M., Arumugam, R., & Paramasivam, S. (2006). Real time implementation of viable torque and flux controllers and torque ripple minimization algorithm for induction motor drive. Energy conversion and management, 47(11-12), 1359-1371. https://doi.org/10.1016/j.enconman.2005.08.013

[13] Mamdouh, M., Abido, M. A., & Hamouz, Z. (2018). Weighting factor selection techniques for predictive torque control of induction motor drives: A comparison study. Arabian Journal for Science and Engineering, 43(2), 433-445. https://doi.org/10.1007/s13369-017-2842-2

[14] Xiao, D., Akter, M. P., Alam, K., Dutta, R., Mekhilef, S., & Rahman, M. F. (2021). Cascaded predictive flux control for a 3-L active NPC fed IM drives without weighting factor. IEEE Transactions on Energy Conversion, 36(3), 1797-1807. doi: 10.1109/TEC.2021.3065648

[15] Bahmani,M . (2026). A Model-Free Predictive Torque Control for Induction Motors Without Weighting Factors. (e738812). Power, Control, and Data Processing Systems, (in press), e738812 doi: 10.30511/pcdp.2026.2093362.1092

[16] Shahid, M. B., Jin, W., Abbasi, M. A., Husain, A. R. B., Munir, H. M., Hassan, M., ... & Alghamdi, T. A. (2024). Model predictive control for energy efficient AC motor drives: An overview. IET Electric Power Applications, 18(12), 1894-1920. https://doi.org/10.1049/elp2.12517

[17] Yang, A., Lu, Z., & Qin, J. (2025). Ultra-local dual-torque model for model-free predictive torque control without weighting factors in induction motor drives. Control Engineering Practice, 160, 106327. https://doi.org/10.1016/j.conengprac.2025.106327

[18] Hassan, M., Zhang, G., Mastoi, M. S., Li, Z., Yu, X., Xu, K., ... & Haris, M. (2025). Optimising weighting factor design for model predictive torque control in IPMSM drives: a grey relational analysis approach. IET Power Electronics, 18(1), e70053. https://doi.org/10.1049/pel2.70053

[19] Zhang, Y., Jia, D., Yin, Z., & Luo, P. (2025). GRA-TOPSIS-based model predictive torque control for induction motor without weighting factors. IEEE Transactions on Power Electronics, 40(9), 12309-12320. DOI: 10.1109/TPEL.2025.3563888

[20] Nguyen, H. V., Pham, H. D., & Pham, D. D. (2026). Weighting-Factor-Free Predictive Torque Control Structures for 3L-NPC Inverter-Fed Induction Motor Drives. IEEE Access. DOI: 10.1109/ACCESS.2026.3656921

[21] Li, C., Meng, Q., & Shi, T. (2024). A review on model predictive control strategies for AC motor drives. IET Electric Power Applications, 18(11), 1584-1604. https://doi.org/10.1049/elp2.12510

[22] Muddineni, V. P., Bonala, A. K., & Sandepudi, S. R. (2016). Enhanced weighting factor selection for predictive torque control of induction motor drive based on VIKOR method. IET Electric Power Applications, 10(9), 877-888. https://doi.org/10.1049/iet-epa.2016.0057

[23] Yami,R Moammer, Soltanizadeh,H and Shahzadi,A . (2026). ML-and VIKOR for Anomaly Detection and Cell Ranking in 5G/B5G. Power, Control, and Data Processing Systems, 3(1), 38-47. doi: 10.30511/pcdp.2025.2072728.1047